Springer

KSME

Journal of Mechanical Science and Technology 26 (10) (2012) 3253~3260
www.springerlink.com/content/1738-494x
DOI 10.1007/s12206-012-0833-5

Performance evaluation and design optimization using differential evolutionary algorithm of the pantograph for the high-speed train †

Jin-Hee Lee[1], Young-Guk Kim[2], Jin-Sung Paik[2] and Tae-Won Park[1,*]

[1]*Department of Mechanical Engineering, Ajou University, Suwon, 443-749, Korea*
[2]*Korea Railway Research Institute, Uiwang, 437-757, Korea*

(Manuscript Received February 2, 2012; Revised June 11, 2012; Accepted June 18, 2012)

Abstract

The global trend in the railway industry is the effort to increase the maximum speed and stability of a train. For an electric railway vehicle to meet this driving performance, stable electric power should be supplied by a catenary system. Various factors affect the current collection performance, most important of which is the dynamic characteristics of a pantograph. In this paper, the sensitivity analysis and design optimization of a pantograph for a high-speed train were conducted using a finite element method. The dynamic catenary-pantograph interaction was analyzed by using the commercial finite element analysis software, SAMCEF. The pantograph was modeled as a three degrees of freedom mass-spring-damper system, and the pre-sag of the contact and messenger wire due to gravity was implemented. The span data of a high-speed line was applied in the analysis model. And the dynamic characteristics of the pantograph model were obtained by a performance test. The reliability of the simulation model was verified by comparing the analysis contact force results with the test data. By simulation, the mean contact force and its standard deviation etc. were evaluated, and then sensitivity of the pantograph was analyzed. Based on the sensitivity analysis results, the specification of the pantograph was optimized. In the optimization process, response surface analysis and differential evolutionary algorithm were applied to define the regressive function and to determine the optimum values for stable current collection performance. Finally, the improvement of the current collection performance was verified by comparing the optimum specification results with the original specification.

Keywords: Catenary; Design of experiments; Differential evolutionary algorithm; High-speed train; Pantograph

1. Introduction

The traction system of a railway vehicle is operated by electric energy supplied by a catenary system, which interacts with the pantograph on the roof of the vehicle. In order to maintain high operating speed of railway vehicles, power must be supplied stably. Even though railway vehicles are operated at high speeds, current collector devices must maintain stable contact conditions and minimize loss of contact, regardless of locomotive vibrations or aerodynamic disturbances. Current collection performance is affected by various factors such as the characteristics of the pantograph, the specifications of an infrastructure like a catenary, operating speed, aerodynamic forces, external forces and other environmental factors. Among them, pantograph characteristics are most related with current collection performance. The high contact forces of the pantograph cause excessive abrasion between the collection plate and the catenary, complicating facility maintenance. On the other hand, low contact forces may cause power supply problems. Normally, train speed is less than 70% of the wave speed of the contact wire. If the vehicle operation speed approaches to the wave speed of the contact wire, the probability of loss of contact is increased. Because of this loss of contact accompanying electric arcs between them, the current collector system becomes seriously damaged. Therefore, it is very important to maintain a stable contact force between the catenary and the collector plate of the pantograph. Especially, to ensure safety at high speeds over 300 km/h, the current collection performance should be pre-evaluated. Because of the increasing interest in high-speed railway vehicles, the dynamic interaction between the catenary and the pantograph at high speeds has been studied extensively.

Catenary/pantograph dynamics has been studied by various methods, which have been classified as analytical methods, approximation methods and modal analysis etc. Currently, the approximation methods such as FEM (finite element method) and FDM (finite differential method) are mainly used to investigate the catenary/pantograph problem because they provide accurate solutions for a wide range of applications. F. Rauter et al. proposed the co-simulation procedure of the catenary

*Corresponding author. Tel.: +82 31 219 2952, Fax.: +82 31 219 1965
E-mail address: park@ajou.ac.kr
† Recommended by Associate Editor Gang-Won Jang

finite element model and the pantograph multibody model [1]. He analyzed the three dimensional behavior and dynamic interaction between the catenary and the pantograph. J. H. Seo et al. analyzed the dynamic interaction between the pantograph and the catenary by applying two-dimensional and three-dimensional finite element absolute nodal coordinates [2, 3]. He used only multibody dynamic analysis technique to implement the model, but the analysis results were not sufficiently evaluated and verified. A. Alberto, A. Collina et al. developed a finite element formulation of a catenary and pantograph. And they analyzed the contact force of the pantograph [4, 5].

In addition to the above developments of analysis models, the factors affecting the dynamic interaction between the catenary and the pantograph were studied. Y. H. Cho investigated the contact force variation due to an initial uplift force of the pantograph and the characteristics of the nonlinear droppers [6]. Also, the relationship among the contact force, pre-sag and velocity of the train was considered. Z. Ning investigated the contact force variation according to the stiffness and damping coefficients of the pan head and the upper frame, tension of the catenary wires and so on [7]. However, he investigated in medium-speeds range and did not consider the changes in masses of pantograph. In order to analyze the sensitivity of the pantograph system, J. W. Kim used an analytical method [8]. He executed state sensitivity analysis with respect to design variables. They employed the 3 DOF pantograph model and contact force was assumed as simple time-varying stiffness model instead of non-linear interaction model. The state equation, which has the form of a first order ordinary differential equation, was derived. In addition, the aerodynamic lift force effect and the length of the span were considered. They investigated the sensitivity of the factors by using the verified pantograph model. However, the catenary and interaction model was insufficient to estimate the behavior of the real system. Also, they did not conduct any optimizations or improvements of the system.

In this paper, using the commercial finite element analysis software SAMCEF, finite element models of a catenary and a pantograph were created and their dynamic interaction at high speeds was evaluated. The specifications of the constructed actual test line were applied to the catenary model in detail. And the pantograph characteristics are obtained and validated by a performance test. By a simulation of high-speed driving, various factors such as the mean contact force and the standard deviation of the contact force were calculated. And the reliability of the analysis model was verified by comparing the analysis results with the measured data obtained from an actual vehicle test. Using this verified finite element model, sensitivity, which is closely associated with contact force variation, was analyzed by applying an experimental method. Based on the results of the sensitivity analysis, design variables and the objective function were re-selected to optimize the pantograph. In the optimization process, the central composite design table and the ANOVA table were applied to determine the regressive model function and to verify it, respectively. Also, a differential evolutionary algorithm was used to obtain the optimum values of the pantograph system. Finally, by comparing the original model to the optimum model, performance improvement was confirmed.

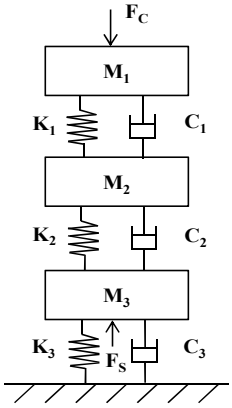

Fig. 1. Three degrees of freedom pantograph model.

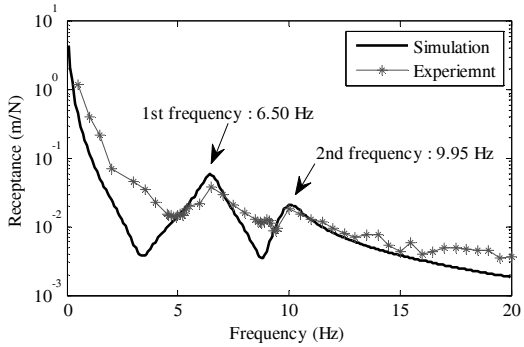

Fig. 2. Receptance of the actual pantograph and simulation model.

2. Finite element analysis model

2.1 Pantograph model

The pantograph is modeled as discrete three degrees of freedom mass-spring-damper system, as shown Fig. 1, instead of an actual complicated kinematic model. To determine the specifications of the three degrees of freedom pantograph model, the characteristics of the vertical vibration of the developed pantograph were obtained by a performance test. A periodic excitation of 0 to 20 Hz was applied to the developed pantograph. Then, using these frequency response characteristics, receptance was defined. The receptance of a pantograph is defined as the ratio between the dynamic vertical displacement of the collector head and dynamic excitation force applied to collector head when the system is excited at specific frequency. This actual receptance was compared with the receptance of the pantograph analysis model, namely the three degrees of freedom discrete mass model. Fig. 2 shows the receptance of the actual pantograph and simulation model. The resonance frequencies of these two results were well

Table 1. Mechanical properties of the pantograph model.

	Mass (kg)	Stiffness (N/m)	Damping (Ns/m)
Upper	$M_1 = 6$	$K_1 = 12{,}340$	$C_1 = 30$
Middle	$M_2 = 12$	$K_2 = 13{,}600$	$C_2 = 0$
Low	$M_3 = 10$	$K_3 = 0$	$C_3 = 64.9$

Table 2. Mechanical properties of the catenary model.

Component	Sectional area (mm^2)	Elastic modulus (GN/m^2)	Line density (kg/m)	Poisson's ratio
Messenger wire	65.49	110	0.605	0.1
Contact wire	150	180	1.334	0.1

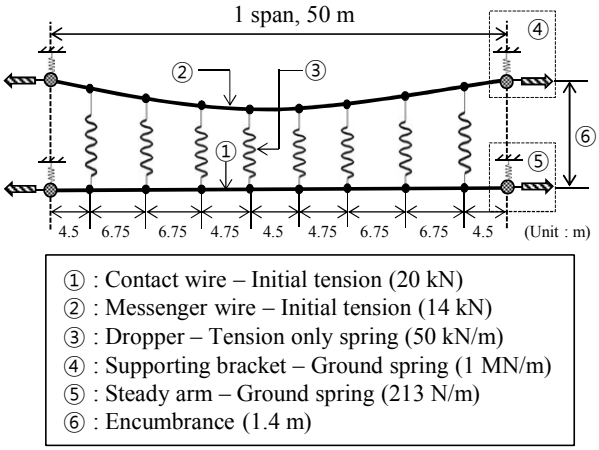

Fig. 3. Description of the catenary system (s50-1).

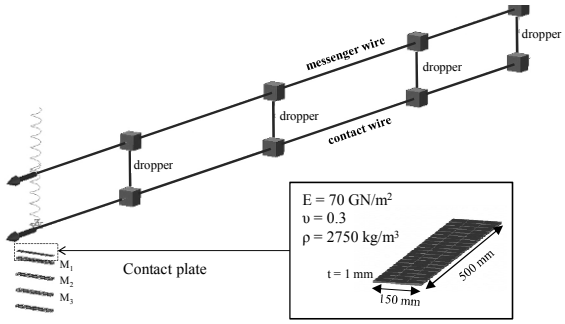

Fig. 4. Finite element model of the catenary and pantograph (initial configuration at t = 0 sec).

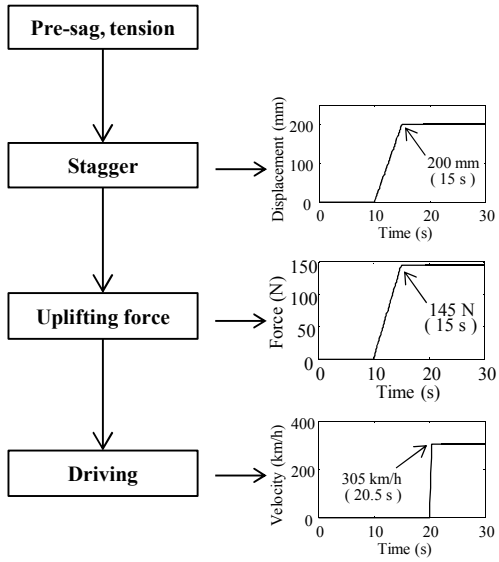

Fig. 5. Simulation procedure.

matched. Through this method, the specifications of the analysis model were obtained. Table 1 shows the specifications of the pantograph model. Detailed pantograph model validation (theory, following performance test, etc.) is described in Ref. [9].

2.2 Catenary model

A simple catenary was used in this paper. The specification of the catenary was same as that of 's50-1', which is the actual operation line constructed in Korea. A catenary system mainly consisted of a contact wire, a messenger wire, and droppers. The length of the one span was 50 m, and a total of 10 spans were modeled for the analysis. The contact and messenger wires were modeled as three dimensional beam elements. Tensions of 20 kN and 14 kN were applied to the end of the contact and messenger wires, respectively. Because the dropper connects the contact and messenger wires vertically and it transfers loads on the contact wire to the messenger wire and then distributes them, it is modeled as a tension only spring. At the end of each span, the supporting brackets supported the whole catenary wires and the steady arm gave a geometric stiffness to the contact wire for stagger. These were modeled using spring element with high and low stiffness, respectively. Fig. 3 shows the catenary system (s50-1). The mechanical properties of the catenary wires are given in Table 2.

3. Analysis and verification of the model

Using the previously mentioned catenary and pantograph models, the dynamic interaction between the two systems at high speed was analyzed as shown in Fig. 4. A driving simulation was carried out by the process shown in Fig. 5. First, from 0 to 10 seconds, in order to implement pre-sag, gravitational force was applied to the catenary wires, which were separated from the pantograph. During that time, the free falling catenary wires will reach their stable shapes by the droppers and supporters (supporting bracket and registration arm). At the same time, tension was applied to the ends of each wire. In the next step, between 10 to 15 seconds, stagger of ±200 mm was applied to the connecting points of the steady arms and the contact wire. The stagger makes a deviation with zigzag pattern from its centerline, so it acts to prevent a concentrated

Table 3. Statistical results of simulation and test.

	Simulation	Test	Error (%)
Mean contact force (N)	144.5	145.8	0.9
Standard deviation (N)	38.5	39.5	2.7
Statistical max. contact force (N)	259.9	264.3	1.7
Statistical min. contact force (N)	29.1	27.3	6.0

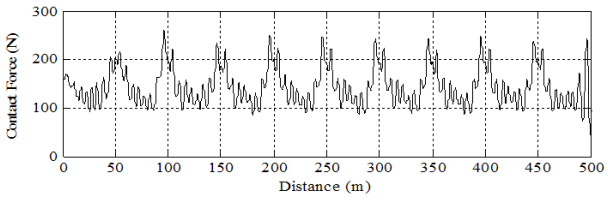

(a)

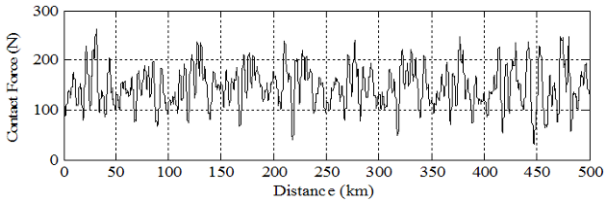

(b)

Fig. 6. Contact force of simulation and test results: (a) Simulation result; (b) On-line test result.

wear of the collector head by dispersing the contact area. In this simulation model, there was no need to consider the wear of the collector head; however, stagger was taken into account to create a model more similar to the real system. Also, in this step, static uplifting force of 145 N was applied to the M_3 of the pantograph. As a consequence, first contact occurs between the pantograph and wire. In order to represent the dynamic interaction between the contact wire and pantograph, 'node to face of an element contact', which is provided in SAMCEF, was employed. The specification of the contact plate is shown in Fig. 4. And the contact force was obtained by calculating the relative reaction force of the high stiffness spring located between the contact plate and the collector head. After the uplifting force was applied for 20 seconds, the pantograph moved along the catenary at 305 km/h, and the contact force was calculated according to time and moving distance. Fig. 6 shows contact force according to moving distance of the simulation model and the measured contact force from a test drive at a real operation line when the vehicle ran at 305 km/h. The on-line driving test for measuring contact forces was performed on 5.5 km section near Pungsegyo in Kyungbu high-speed line. The measured data was provided by Korea Railroad Research Institute. Results were filtered from 0 to 20 Hz by a low pass filter. The 6 order Butterworth filter proven in MATLAB was used for low pass filtering. In the case of the simulation results, contact force increased at the end of each span, periodically. On the other hand, in the case

Table 4. Design variables of the pantograph.

Design variables	Unit	Level	
		Min (-1)	Max (+1)
M_1	kg	5.4	6.6
M_2	kg	10.8	13.2
M_3	kg	9.0	11.0
K_1	N/m	11,106	13,574
K_2	N/m	12,240	14,960
C_3	Ns/m	58.4	71.4

of the test results, though some periodical behavior occurred, the measured contact force variation behaved irregularly. However, the statistical results represented in Table 3, such as the mean contact force (σ), the standard deviation of the contact force (F_m), the statistical maximum and minimum contact forces ($F_m \pm 3\sigma$), were well matched between the simulation and test. In general, in the evaluation of current collection performance, the quantitative values in Table 3 are more important than the shape of the contact force variation according to distance or time. Through this comparison, the catenary and pantograph finite element model was verified.

4. Sensitivity analysis

Using the verified finite element model, sensitivity analysis was conducted to understand influence of the pantograph design variables on the mean value (F_m) and standard deviation of the contact force (σ). Six of the nine design variables of the three degrees of freedom pantograph model, which were considered to be important, were selected for sensitivity analysis. Among the numerical, analytical and experimental methods of sensitivity analysis, the experimental method was employed in this paper [10]. Table 4 represents the design variables and their levels. A two level factor was used for experiments. And the boundary of the each level were determined as $\pm 10\%$ of the initial specification by engineering discussion. The Plackett-Burman design table was applied by assuming no interaction. As described above, the mean value and standard deviation of the contact force were considered as the objective functions. The driving scenario of the pantograph model is to pass 10 spans of catenary wires (s50-1 type) at 305 km/h. The contact force generated from the 5th span to the 6th span are filtered and statistically processed. The 12-run Plackett-Burman design table and the experimental results are shown in Table 5.

Using the analysis results of two level experiments, two response surfaces for the two objective functions were estimated. The coefficients of the response surfaces were obtained by multiplying the pseudo-inverse of the coefficient matrix with the resultant matrix. These coefficients mean the change of the results of the objective function due to the change of design variables. As shown in Table 5, the mean contact force is not factor that changes due to the pantograph specification. The mean contact force is affected by only the static uplifting force

Table 5. 12-run Plackett-Burman design table.

No.	M_1	M_2	M_3	K_1	K_2	C_3	F_m	σ
1	1	1	-1	1	1	1	144.6891	39.3023
2	-1	1	1	-1	1	1	144.7655	38.7913
3	1	-1	1	1	-1	1	144.7172	38.9846
4	-1	1	-1	1	1	-1	144.6598	37.5979
5	-1	-1	1	-1	1	1	144.7199	37.3036
6	-1	-1	-1	1	-1	1	144.6686	35.2233
7	1	-1	-1	-1	1	-1	144.6600	39.1620
8	1	1	-1	-1	-1	1	144.7360	39.9970
9	1	1	1	-1	-1	-1	144.8168	41.9883
10	-1	1	1	1	-1	-1	144.7532	38.9813
11	1	-1	1	1	1	-1	144.6794	39.6771
12	-1	-1	-1	-1	-1	-1	144.6665	36.4953

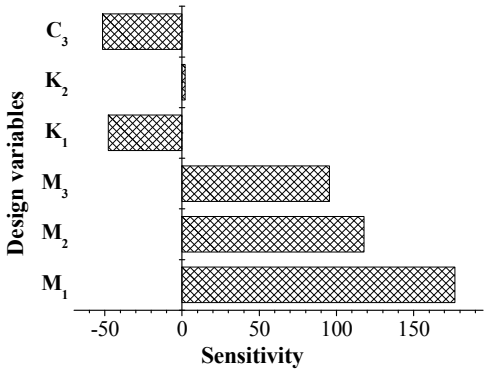

Fig. 7. Result of sensitivity analysis for standard deviation of contact force.

and the aerodynamic force. Thus, the mean contact force was excluded in the optimization. On the other hand, the standard deviation of the contact force is affected by the specification of the pantograph. Eq. (1) is the regressive model function and Fig. 7 shows the result of sensitivity analysis with respect to the standard deviation of the contact force. M_1 was the most sensitive parameter, followed by M_2, M_3, C_3, K_1, and K_2. Because less contact force deviation means more stable current collection performance, the contact force deviation needs to be minimized to improve the collection performance.

$$y_\sigma = 5.5621e3 + 176.6220M_1 + 117.7460M_2 + 95.3807M_3 - 47.6546K_1 + 1.9704K_2 - 51.5980C_3 \quad (1)$$

5. Design optimization

5.1 Regressive model function

Based on the results of the sensitivity analysis, current collection performance was optimized. A total of five design variables (M_1, M_2, M_3, K_1, and C_3) were selected. K_2 was excluded due to its small influence. Because less contact force deviation means more stable performance, the minimization of the standard deviation of the contact force was chosen as the objective function. The boundary of each design variable is as shown in Table 4. Appendix 1 provides the central composite design table, which has five factors and one center point. Using this design table, a total of 43 experiments were executed. Eq. (2) is the estimated regressive model function.

Table 6. Analysis of variance (ANOVA) table.

Factor	S	Φ	V	F_0	F(0.01)
Regression variable	102.731	5	20.546	3.08e5	4.43
Residual variation	0.003	37	6.7e-5		
Sum	102.734	42			

$$\begin{aligned} y = {} & 38.6002 + 1.2135M_1 + 0.7920M_2 + 0.6570M_3 - 0.3436K_1 \\ & - 0.3417C_3 + 0.0339M_1^2 - 0.0152M_2^2 - 0.0094M_3^2 - 0.0024K_1^2 \\ & + 0.0099C_3^2 - 0.0113M_1M_2 - 0.0237M_2M_3 + 0.0084M_3K_1 \\ & + 0.0143K_1C_3 - 0.0176M_1M_3 + 0.0018M_2K_1 - 0.0126M_3C_3 \\ & - 0.0363M_1K_1 - 0.0068M_2C_3 - 0.0028M_1C_3 \end{aligned} \quad (2)$$

Table 6 is the ANOVA table that was used to verify reliability of the regressive model. In this table, S, phi and V are the size of change, degree of freedom, and mean square, respectively. Also, F_0 is the value obtained from the experiments and F(0.01) is a value referred F-distribution. As shown in Table 6, F_0 is greater than F(0.01). This means that the estimated regressive model function has reliability in the 99 percent of the confidence intervals. Therefore, this regressive model function can be used as the objective function.

5.2 Differential evolutionary algorithm

In order to determine the optimum values of the design parameters, various optimization algorithms can be used depending on the type of objective function and constraints. In this paper, a differential evolutionary algorithm was employed. The differential evolutionary algorithm, suggested by Rainer Storn and Kenneth Price [11], is an optimization algorithm that can extract the minimum value in a design space [12]. It is a novel parallel direct search method, which utilizes NP parameter vectors of Eq. (3) as the population for each generation G,

$$\underline{\mathbf{x}}_{i,G} = x_{ij,G} \quad (i = 1, 2, \cdots, NP \quad j = 1, 2, \cdots, NS) \quad (3)$$

where NP is the population size and NS is the number of parameters to search. NP does not change during the minimization process. If nothing is known about the system, the initial population is chosen randomly. As a rule, a uniform probability distribution is assumed for all random decisions. If a pre-

liminary solution is available, the initial population is often generated by adding normally distributed random deviations to the nominal solution $\underline{\mathbf{x}}_{nom,0}$.

The main idea behind DE is the new scheme for generating trial parameter vectors. DE generates new parameter vectors by adding the weighted difference vector between two population members to the vector of a third member. If the resulting vector yields a lower objective function value than that from the vector of a predetermined population member, the newly generated vector replaces the vector with which it was compared. For each vector, $\underline{\mathbf{x}}_{i,G}$, a trial vector $\underline{\mathbf{v}}_{i,G}$ is generated according to Eq. (4),

$$\underline{\mathbf{v}}_{i,G} = \underline{\mathbf{x}}_{r_1,G} + F \cdot (\underline{\mathbf{x}}_{r_2,G} - \underline{\mathbf{x}}_{r_3,G}) \tag{4}$$

with $r_1, r_2, r_3 \in [1, NP]$, integer and mutually different, and $F > 0$.

The mutually different integers r_1, r_2 and r_3 are chosen randomly with uniform distribution from the interval (1, NP), and they are also different from the running index *i*. F is a real and constant factor which controls the amplification of the differential variation $(\underline{\mathbf{x}}_{r_2,G} - \underline{\mathbf{x}}_{r_3,G})$. In order to increase the diversity of the parameter vectors, a vector is formed as in Eq. (5),

$$\underline{\mathbf{u}} = (\underline{\mathbf{u}}_1, \underline{\mathbf{u}}_2, \cdots, \underline{\mathbf{u}}_{NP})^T \tag{5}$$

with

$$\underline{\mathbf{u}}_j = u_{ji} = \begin{bmatrix} v_{ji} \ if (rand \le Cr) \\ x_{ji,G} \quad otherwise \end{bmatrix} \quad j = 1, \cdots, NP \quad i = 1, \cdots, NS$$

where *rand* is a random number generated with uniform distribution in the range from 0 to 1 and *Cr* is a crossover rate.

5.3 Optimization results

Using the previously mentioned regressive model and the differential evolutionary algorithm, the optimization to minimize the standard deviation of the contact force was conducted. Consequently, the optimal values of the pantograph specifications could be obtained. Table 7 shows the original and optimum values of each design variable. M_1, M_2 and M_3 are determined as the values of the upper boundary, and K_1, C_3 are determined as the values of the lower boundary. At the speed of 305 km/h, the standard deviation of the contact force was reduced by about 9 percent. As you can see, the optimal pantograph has high resonant frequencies than the original pantograph. It is noticeable that modification of 10% is very hard for mass, but easy for stiffness. So, as an additional study, to obtain better performance, the standard deviation of the contact force was evaluated according to the increased stiffness (K_1) in given optimum specification. Table 8 shows the result of the evaluation. The standard deviation of the contact force was decreased as the stiffness increases but, rate of decrease was very small. It was expected results because sensitivity of K_1 is relatively small. And to conclusion, smaller mass and larger stiffness is better to decrease standard deviation of the contact force in manufacturing limitations.

Table 7. Original and optimum values of the design variables.

Design variables	Unit	Original	Optimum
M_1	kg	6.0	5.4
M_2	kg	12.0	10.8
M_3	kg	10.0	9.0
K_1	N/m	12340	13574
C_3	Ns/m	64.9	71.4
Result (σ)	N	38.6042	35.2837

Table 8. Analysis results according to the increase of stiffness (K_1).

Rate of increase	10% (optimum)	30%	50%	70%	100%
Stiffness	13574	16042	18510	20978	24680
Result (σ)	35.28	34.78	34.43	34.40	34.38

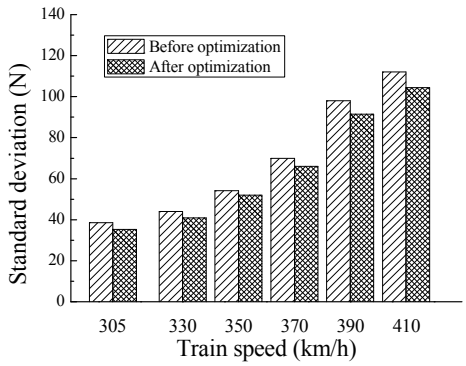

Fig. 8. Standard deviation of contact force of the original and optimum designs (V = 305 km/h to 410 km/h).

Using the original and optimum pantograph models, high-speed driving simulation at various velocities was carried out. Fig. 8 shows the standard deviations of the contact forces of the original and the optimum design at train speeds of 305 to 410 km/h. Also, Fig. 9 shows the statistical minimum and maximum contact forces at the same velocity. The optimal pantograph provides more stable current collection performance than the original pantograph over the entire speed range. This result shows that the optimization was performed successfully [13]. The international standard EN 50119 includes the requirements of current collection systems [14]. In this standard, the statistical maximum contact force must be less than 350 N at high speeds over 200 km/h. On the other hand, the statistical minimum contact force, which is used to determine the no loss of contact between the pantograph and the overhead contact line, should be positive. According to this international standard, the current collection system consid-

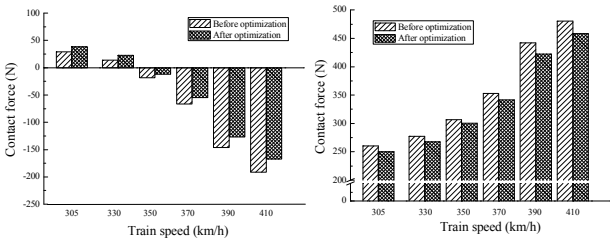

(a) Statistical min. (F_m-3σ) (b) Statistical max. (F_m+3σ)

Fig. 9. Statistical minimum and maximum contact forces of the original and optimal designs (V = 305 km/h to 410 km/h).

ered in this paper should not be operated over 350 km/h. In UIC code 799 OR, wave propagation of a catenary is defined as $C = \sqrt{(T_m+T_c)}/\sqrt{(\rho_m+\rho_c)}$, where, T is the tension and ρ is line density and subscripts c and m denote the contact and messenger wire, respectively [15]. As mentioned previously, the contact force is dominated by the wave propagation speed in the high-speed. Therefore, the performance of this system will be improved by increasing the tensions of the catenary wires.

6. Conclusion

In this paper, using a three dimensional finite element catenary-pantograph numerical model, performance evaluation and design optimization of the pantograph were carried out. The catenary was modeled as a beam element, and the pre-sag analysis was performed. Also, the pantograph was assumed as a discrete mass-spring-damper model to reflect the frequency characteristics of an actual kinematic pantograph. By simulation of driving at the high speed of 305 km/h, the contact force was calculated. Also, the analysis model was verified by comparing the simulation results with actual test results. Using this verified simulation model, sensitivity analysis was performed, and the design variables and objective function were evaluated and re-selected. And then to minimize the standard deviation of the contact force, an optimization process, which applied the response surface analysis method and the differential evolutionary algorithm, was carried out. Finally, by comparison of the original and optimum pantograph models, it was shown that the optimum pantograph provided more stable performance than the original pantograph over the entire speed range.

In the future, using these results, an optimal actual kinematic pantograph will be developed. In addition, for further improve the current collection performance, the influence of the other parameters such as catenary specifications will be considered.

Acknowledgment

The work described in this paper was performed within the Next-Generation High Speed Rail Technology Development Project, being funded and Promoted by MLTM (The Minister of Land, Transport and Maritime Affairs).

References

[1] F. Rauter and J. Ambrosio, Contact model for the pantograph-catenary interaction, *Journal of System Design and Dynamics*, 1 (3) (2007) 447-457.

[2] J. W. Seo and T. W. Park, Dynamic analysis of a pantograph-catenary system using absolute nodal coordinates, *Vehicle System Dynamics*, 44 (8) (2006) 615-630.

[3] J. W. Seo and T. W. Park, Three-dimensional large deformation analysis of the multibody pantograph/catenary systems, *Nonlinear Dynamics*, 42 (2005) 199-215.

[4] A. Alberto and J. Benet, A high performance tool for the simulation of the dynamic pantograph-catenary interaction, *Mathematics and Computers in Simulation*, 79 (2008) 652-667.

[5] A. Collina and S. Bruni, Numerical simulation of pantograph-overhead equipment interaction, *Vehicle System Dynamics*, 38 (4) (2002) 261-291.

[6] Y. H. Cho, Numerical simulation of the dynamic responses of railway overhead contact lines to a moving pantograph, considering a nonlinear dropper, *Journal of Sound and Vibration*, 315 (2008) 433-454.

[7] N. Zhou and W. Zhang, Investigation on dynamic performance and parameter optimization design of pantograph and catenary systems, *Finite Elements in Analysis and Design*, 47 (2011) 288-295.

[8] J. W. Kim and H. C. Chae, State sensitivity analysis of the pantograph system for a high-speed rail vehicle considering span length and state uplift force, *Journal of Sound and Vibration*, 303 (2007) 405-427.

[9] S. P. Jung and T. W. Park, Analysis of the current-collection performance of a high-speed train using finite element analysis method, *Transactions of Korean Society of Mechanical Engineers A*, 35 (7) (2011) 827-833.

[10] S. P. Jung and T. W. Park, A study on the optimization method for a multi-body system using the response surface analysis, *Journal of Mechanical Science and Technology*, 23 (2009) 950-953.

[11] K. Price and R. Storn, Differential evolution: Numerical optimization made easy, *Dr. Dobbs Journal* (1997) 18-24.

[12] Y. G. Kim and C. K. Park, Design optimization for suspension system of high speed train using neural network, *JSME International Journal : series C*, 46 (2) (2003) 727-735.

[13] J. S. Paik, Dynamic performance evaluation and parameter optimization of the current collection system for the high-speed vehicle, *Dissertation, Inha University* (2012).

[14] European committee for electrotechnical standardization EN 50119:2001, Railway Applications-Fixed Installations-Electric Traction Overhead Contact Line (2001).

[15] UIC Code 799 OR, Characteristic of a.c. overhead contact systems for high-speed lines worked at speeds of over 200 km/h (2002).

Appendix

A.1 Central composite design table and simulation results

No.	M_1	M_2	M_3	K_1	C_3	Standard deviation (σ)
1	1	1	1	1	1	40.5311
2	1	1	1	1	-1	41.2196
3	1	1	1	-1	1	41.2061
4	1	1	1	-1	-1	41.9681
5	1	1	-1	1	1	39.2728
6	1	1	-1	1	-1	39.9222
7	1	1	-1	-1	1	40.0286
8	1	1	-1	-1	-1	40.7441
9	1	-1	1	1	1	38.9960
10	1	-1	1	1	-1	39.6676
11	1	-1	1	-1	1	39.7220
12	1	-1	1	-1	-1	40.4574
13	1	-1	-1	1	1	37.6893
14	1	-1	-1	1	-1	38.3079
15	1	-1	-1	-1	1	38.4432
16	1	-1	-1	-1	-1	39.1181
17	-1	1	1	1	1	38.2058
18	-1	1	1	1	-1	38.8998
19	-1	1	1	-1	1	38.7850
20	-1	1	1	-1	-1	39.5297
21	-1	1	-1	1	1	36.9249
22	-1	1	-1	1	-1	37.5623
23	-1	1	-1	-1	1	37.5292
24	-1	1	-1	-1	-1	38.2183
25	-1	-1	1	1	1	36.6628
26	-1	-1	1	1	-1	37.3332
27	-1	-1	1	-1	1	37.2532
28	-1	-1	1	-1	-1	37.9602
29	-1	-1	-1	1	1	35.2838
30	-1	-1	-1	1	-1	35.8964
31	-1	-1	-1	-1	1	35.8699
32	-1	-1	-1	-1	-1	36.5418
33	0	0	0	0	0	38.6042
34	-1.596	0	0	0	0	36.7504
35	1.596	0	0	0	0	40.6212
36	0	-1.596	0	0	0	37.2967
37	0	1.596	0	0	0	39.8247
38	0	0	-1.596	0	0	37.5330
39	0	0	1.596	0	0	39.6181
40	0	0	0	-1.596	0	39.1401
41	0	0	0	1.596	0	38.0466
42	0	0	0	0	-1.596	39.1671
43	0	0	0	0	1.596	38.0822

Jin Hee Lee received his B.S degree in Mechanical Engineering from Ajou University in 2009. Currently he is a Ph.D. candidate at Ajou University in Suwon, Korea. Mr. Lee's research interests are in the area of flexible multi-body dynamic and computer aided engineering.

Tae Won Park received his B.S degree in Mechanical Engineering from Seoul National University. He then went on to receive his M.S. and Ph.D. degrees from the University of Iowa. Dr. Park is currently a Professor at the School of Mechanical Engineering at Ajou University in Suwon, Korea.